International Journal of GEOMATE, Dec., 2025 Vol.29, Issue 136, pp.104-112
ISSN: 2186-2982 (P), 2186-2990 (O), Japan, DOI: https://doi.org/10.21660/2025.136.g14221
Geotechnique, Construction Materials and Environment

EVALUATION OF RETAINING WALL COLLAPSE RISK UTILIZING VIBRATION CHARACTERISTICS

Yudai Harima[1], *Taichi Hyodo[2], Hiroki Fujita[3], Lin Wang[4] and Shangning Tao[4]

[1]Oriental Consultants Corporation, Japan, [2]Toyama Prefectural University, Japan,
[3]Toyama City, Japan, [4]Chuo Kaihatsu Corporation, Japan

*Corresponding Author, Received: 22 July 2025, Revised: 16 Nov. 2025, Accepted: 18 Nov. 2025

ABSTRACT: Since 1955, Japan has experienced a period of rapid economic growth, during which various social infrastructure facilities were constructed. Recently, however, the aging of these infrastructures has become a significant issue. Inspection and maintenance are essential for the upkeep of these infrastructure facilities. Currently, visual inspections are the mainstream method, making it challenging to quantitatively identify damage. In this study, vibration sensors were installed at the base and top sections of retaining walls, and vibrations from adjacent trains were utilized to evaluate the collapse risk of the retaining walls based on their vibration characteristics. The vibration characteristics were quantitatively assessed by calculating the primary natural frequency from the transfer function and observing temporal changes in the natural frequency to determine the degree of deterioration of the retaining walls. The analysis results showed no significant changes in the vibration characteristics of the retaining walls, indicating no collapse risk. By understanding the inherent vibration characteristics of the retaining walls, it is possible to perform quantitative evaluations, which may be applicable in determining the presence of damage and the necessity of countermeasures in the event of a disaster.

Keywords: Retaining Wall, Monitoring, Natural Frequency, Vibration Sensor

1. INTRODUCTION

Since 1955, Japan has undergone a period of rapid economic growth, during which a wide range of social infrastructure facilities such as bridges and tunnels were constructed. In recent years, however, the aging of these infrastructures has become a serious social issue. According to the Ministry of Land, Infrastructure, Transport and Tourism, it is estimated that by the year 2040, 75% of all bridges, 52% of tunnels, and 65% of port quay facilities will have exceeded 50 years since construction [1].

Given the accelerated deterioration of infrastructure, routine inspection and maintenance are essential. In Japan, visual inspection remains the mainstream method. However, visual inspection requires securing sufficient labor and ensuring the safety of inspectors. Furthermore, it is difficult to quantitatively assess the degree of risk posed by structural damage based on human judgment alone. These inspections also rely heavily on the skills and experience of the workers. Considering Japan's aging population and declining birthrate, the shortage of skilled successors is becoming a serious concern.

Therefore, in the future of Japan's construction industry, there is a growing need for technologies that allow accurate, rapid, and easily accessible assessment of structural degradation for effective infrastructure maintenance. In recent years, advanced technologies such as Artificial Intelligence (AI) and Information and Communication Technology (ICT) have become more prevalent. It is essential to establish a cost-effective and high-quality maintenance system by integrating these technologies.

In response, the authors developed a system that incorporates ICT technologies—such as vibration sensors and mobile communication systems—to monitor site conditions in real time, aiming to assess the structural health of infrastructure.

For bridges and earth structures, Structural Health Monitoring (SHM) using the vibration characteristics of the structure has attracted attention as a solution to problems such as labor shortages, safety risks, and inspection accuracy [2-6]. Nishimura and Haya (1991) developed an impact vibration testing method using natural frequency as an indicator to assess the health of underground foundation structures, which cannot be visually inspected directly [3]. They reported that by understanding the initial natural frequency of a structure and then re-evaluating it after events such as earthquakes, the most appropriate health assessment can be performed based on changes in natural frequency.

Nakajima, Ehara, and Abe (2016) evaluated the applicability of impact vibration testing for diagnosing the health of old earth-retaining walls [4]. They showed that by using velocity sensors to obtain spectral waveforms, the spectral area and spectral score can serve as indicators for detecting stability-related deformations, monitoring their progression, and evaluating the effectiveness of reinforcement.

Many other studies have been conducted in which structural health is assessed by applying impacts to structures and analyzing their vibration response

characteristics. More recently, studies utilizing ambient microtremors have also been reported [7-10].

On the other hand, Ogata, Matsuyama, and Amano (2003) proposed a method for quantitatively and objectively evaluating the potential risk of falling for scattered boulders and floating stones located on slopes [11]. Based on a comprehensive evaluation of laboratory simulations and field measurements, they demonstrated that three vibration characteristics—dominant frequency, damping ratio, and RMS velocity amplitude ratio—are effective indicators for assessing rockfall risk. Furthermore, they presented a rockfall hazard evaluation diagram with threshold values for each of these parameters, which enables the classification of areas into stable and unstable zones.

In this study, we aim to evaluate the structural health of a retaining wall that includes a construction joint by analyzing changes in its vibration characteristics. Vibration sensors were installed on both the upper and lower parts of the construction joint, and vibrations induced by passing trains were used as excitation sources. Moreover, by applying the hazard assessment method proposed by Ogata, Matsuyama, and Amano, and considering the jointed portion of the retaining wall analogously to a potential falling rock, we attempted to quantitatively assess the collapse risk of the wall using the three vibration indicators: natural frequency, damping ratio, and RMS velocity amplitude ratio.

2. RESEARCH SIGNIFICANCE

This study proposes a structural health monitoring method that is simpler to implement and more cost-effective than conventional impact vibration testing approaches. Unlike traditional methods, the proposed approach enables long-term observation of structural health variations through continuous data acquisition. In addition, by employing three vibration characteristics—natural frequency, damping ratio, and RMS velocity amplitude ratio—this method allows for a quantitative assessment of the correlation between structural deterioration and each parameter, thereby enhancing diagnostic accuracy.

3. TARGET RETAINING WALL AND MEASUREMENT OVERVIEW

3.1 Target Retaining Wall

The retaining wall under observation is in a mountainous area of Toyama City, Toyama Prefecture, Japan. As shown in

Fig. **1**, the retaining wall is adjacent to both a road and a railway. Therefore, if the retaining wall were to collapse, it could potentially disrupt train operations. Furthermore, rugged mountain slopes run alongside the road, and locations suspected to be landslide blocks have been identified near the retaining wall. The collapse of the retaining wall could lead to the failure of such landslide-prone slopes.

Fig. **2** shows the front view of the retaining wall, where a diagonal construction joint can be observed. Additionally, fine cracks were identified on the retaining wall closer to the observer.

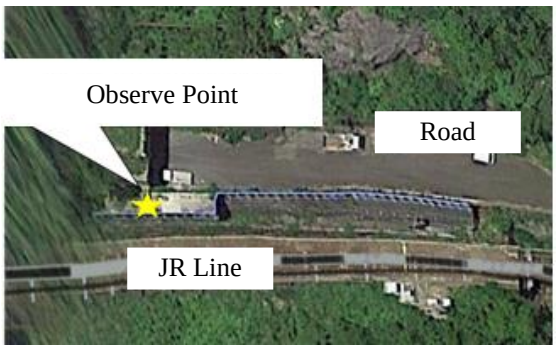

Fig. 1 Observation Point

Fig. 2 Target Retaining Wall

3.2 Measurement Overview

In this study, we used train-induced vibrations to quantitatively measure the deterioration of a retaining wall by analyzing changes in its vibration characteristics, to assess the wall's health (stability). To conduct the measurements, we employed MEMS-type accelerometer sensors owned by Chuo Kaihatsu Corporation. The accelerometer sensors were installed at two locations: the lower side of the retaining wall (No.1) and the upper surface of the retaining wall (No.2), to measure acceleration

waveforms during train operations and seismic events. To measure input and response vibrations, the accelerometer at measurement points No.1 was fixed to the foundation of the retaining wall, and the results were compared with those from the accelerometer installed at the upper surface (No.2) to calculate the response amplification ratio of the retaining wall. Each accelerometer (No.1 and No.2) continuously recorded three-axis components (NS, EW, UD) at a sampling rate of 125 Hz. Acceleration waveforms were output when the measured acceleration exceeded a predefined threshold (2.0 gal), allowing us to assess the differences in vibration magnitudes between the upper and lower measurement points. Additionally, during the measurements, data transfer was conducted via LTE (Long Term Evolution) communication, a mobile phone communication standard.

In this study, the analysis used vibration records from two periods: train-induced vibrations recorded from April 25 to August 1, 2022, and vibration records from the 2023 Noto earthquake (Mj 5.9) that occurred at approximately 21:58 on May 5, 2023, with its epicenter in Suzu City, Ishikawa Prefecture.

A) Top Installation

B) Bottom Installation

Fig. 3 MEMS Type Acceleration Vibration Sensor

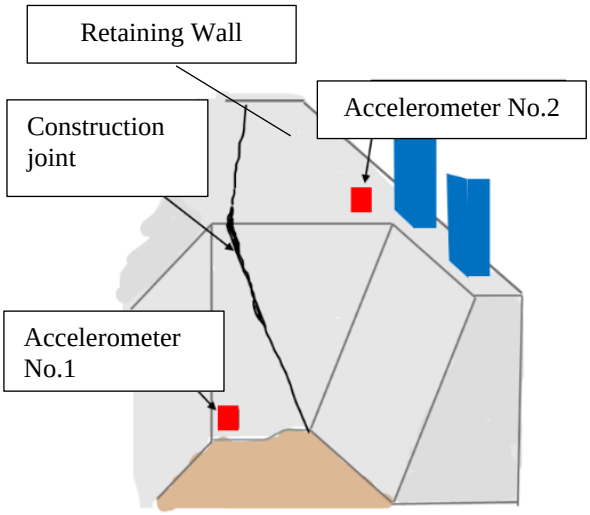

Fig. 4 Acceleration Vibration Sensor Installation Location

4. ANALYSIS OVERVIEW

4.1 Acceleration Waveform Records

Fig. 5 (A), (B), and (C) present the train-induced vibration waveforms recorded on May 1, 2022, by Acceleration Sensor No. 2, installed at the top of the retaining wall, and Acceleration Sensor No. 1, installed at the base of the wall. The waveforms correspond to the NS (north–south), EW (east–west), and UD (up–down) components. In all components, the base of the retaining wall exhibited higher acceleration responses than the top

Fig. **6** (A), (B), and (C) show the vibration waveforms recorded during the 2023 Noto Earthquake (Mj 5.9) on May 5, 2023, at 21:58, using the same sensors and directional components. Unlike the train-induced vibrations, the seismic motion resulted in greater acceleration responses at the top of the retaining wall compared to the base.

This contrasting behavior is attributed to the fundamental differences in the nature of the two types of excitement. Train-induced vibrations are typically short in duration and consist mainly of surface waves, which propagate near the ground surface and attenuate rapidly. As a result, the acceleration amplification at the top of the retaining wall is relatively small. In contrast, seismic waves generated by earthquakes originate from deep underground bedrock layers and tend to amplify as they approach the surface. This amplification effect likely led to the increased acceleration observed at the top of the retaining wall during the earthquake.

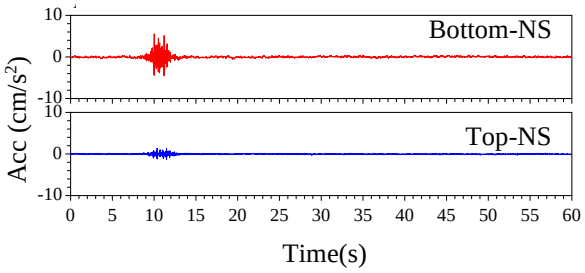

A) 2022/05/01-NS

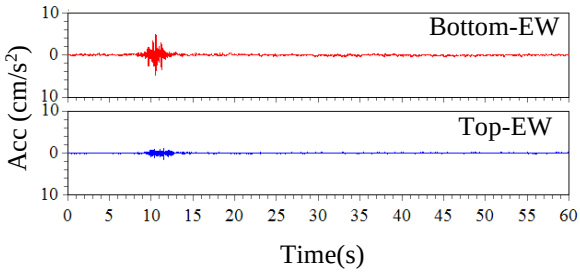

B) 2022/05/01

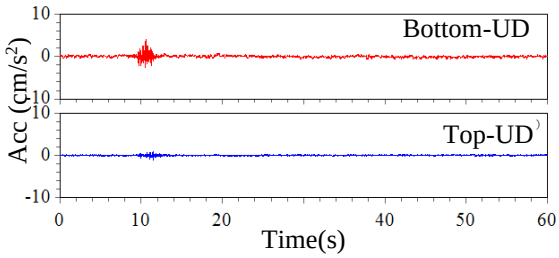

C) 2022/5/01-UD

Fig. 5 Acceleration waveform data (when train passes)

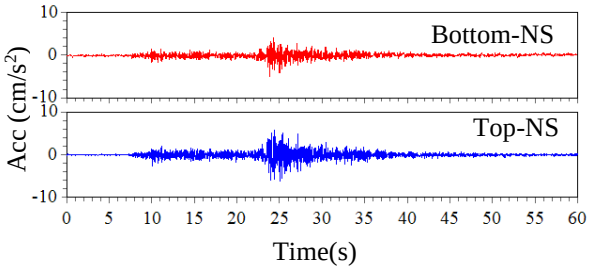

A) 2023/05/05-NS

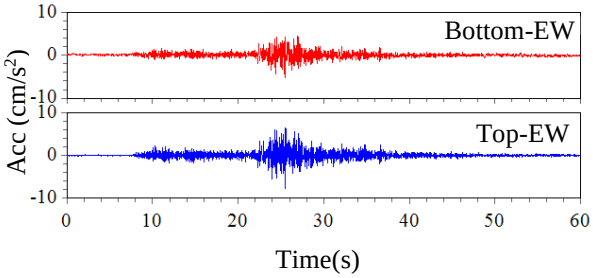

B) 2023/05/05-EW

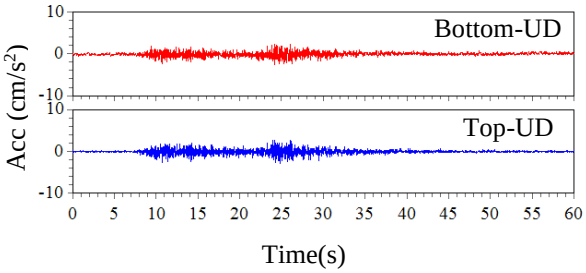

C) 2023/05/05-UD

Fig. 6 Acceleration Waveform Data (during the 2023 Noto Earthquake)

4.2 Displacement Trajectory

The displacement waveform trajectories during vibrations were derived from the acceleration waveforms obtained by the sensors. Comparing the displacement waveforms from train-induced vibrations on May 1, 2022, and the Noto swarm earthquake on May 5, 2023, it was observed that the displacement at the base of the retaining wall was greater than at the top in both cases. Additionally, the displacement trajectories revealed that during both the train-induced vibrations and the Noto swarm earthquake, the retaining wall swayed primarily in the NW-SE direction.

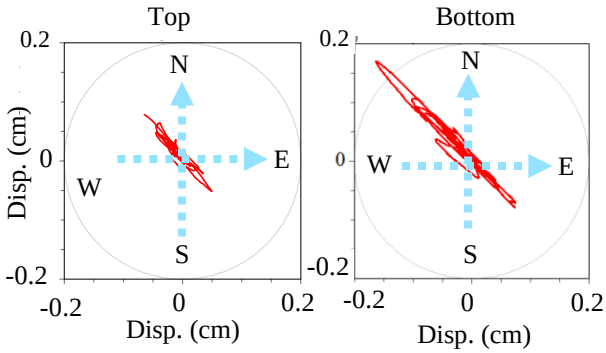

Fig. 7 Trajectory of Displacement (during train vibration)

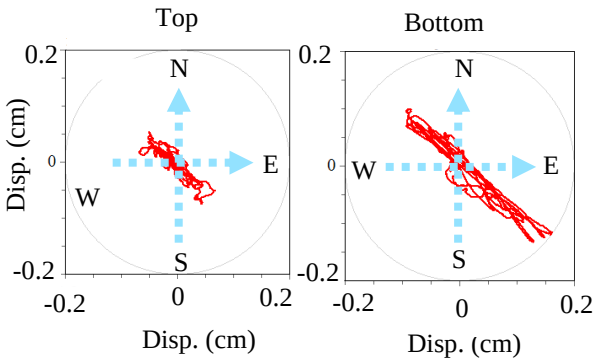

Fig. 8 Trajectory of Displacement (2023 Noto Earthquake)

4.3 Calculation of the Transfer Function

The Fourier spectrum in the frequency domain was determined through FFT (Fast Fourier Transform) based on acceleration waveforms obtained from the sensors placed on the base and the top surface of the retaining wall. Using the derived Fourier spectrum, the frequency response function was calculated. During this process, a window function was applied to smooth the signals. The ratio of output to input at specific frequency components was calculated to derive the transfer function of the retaining wall. Additionally, to evaluate the damping constant, the $1/\sqrt{2}$ method was employed. This method provides a simple evaluation of damping characteristics by using the half-power points of the vibration response at the primary natural frequency. The equation is provided below.

$$\zeta = \frac{f_2 - f_1}{2f_r} \quad (1)$$

Here,
ζ: Damping ratio, f_1, f_2: Frequencies corresponding to the amplitude at $\sqrt{2}/2$ of the maximum amplitude,
f_r : Frequency at which the maximum amplitude occurs

4.3.1 The recorded data from 2022/05/01 and 2022/08/01 (vibration waveforms during typical train passage)

Fig. 9-11 shows the Fourier amplitude spectrum ratio (upper graph) and Fourier phase spectrum ratio (lower graph) of response amplification for the NS component (Fig. 9), EW component (Fig. 10), and UD component (Fig. 11) on May 1, 2022, and August 1, 2022. The Fourier amplitude spectrum represents the intensity of each frequency component in the frequency domain, while the Fourier phase spectrum shows the phase difference for each frequency component. From the Fourier amplitude spectra of the NS and EW components, prominent frequencies appear as multiple natural frequencies. The authors evaluated the first natural frequency of the retaining wall as 12 Hz at this point. The UD component, unlike the NS and EW components, exhibited a gentle, hump-shaped waveform around 22 Hz. The authors considered the 22 Hz peak in the UD component to represent its natural frequency. Although this paper presents data from May 1, 2022, and August 1, 2022, the data during the measurement period for the NS, EW, and UD components showed very similar results. Additionally, the significant fluctuations in the phase spectrum are believed to be caused by the complex vibrations from the train, which include various types of noise, leading to unstable resonant conditions and, consequently, the rapid variations in the phase spectrum.

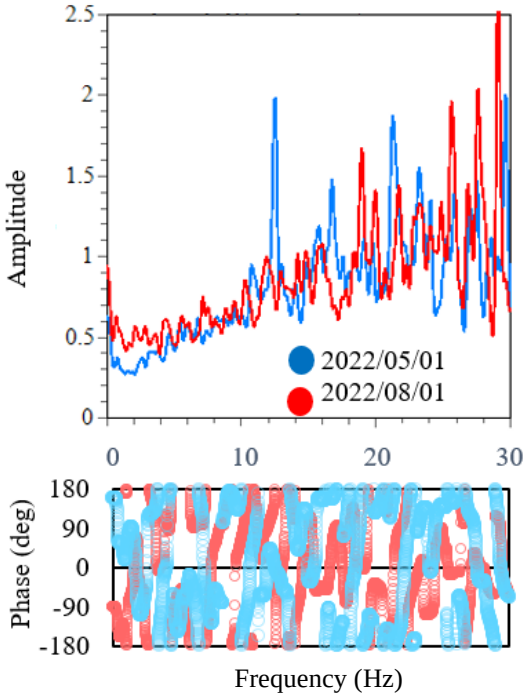

Fig. 9 Fourier amplitude spectrum ratio (upper graph) and Fourier phase spectrum ratio (lower graph)-NS direction

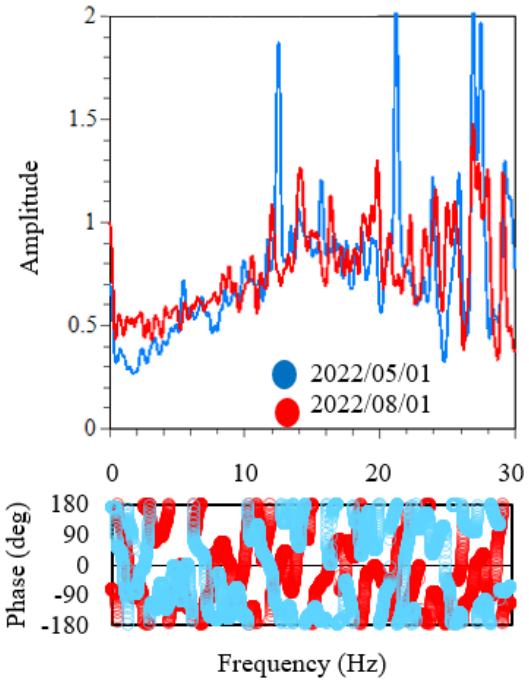

Fig. 10 Fourier amplitude spectrum ratio (upper graph) and Fourier phase spectrum ratio (lower graph)-EW direction

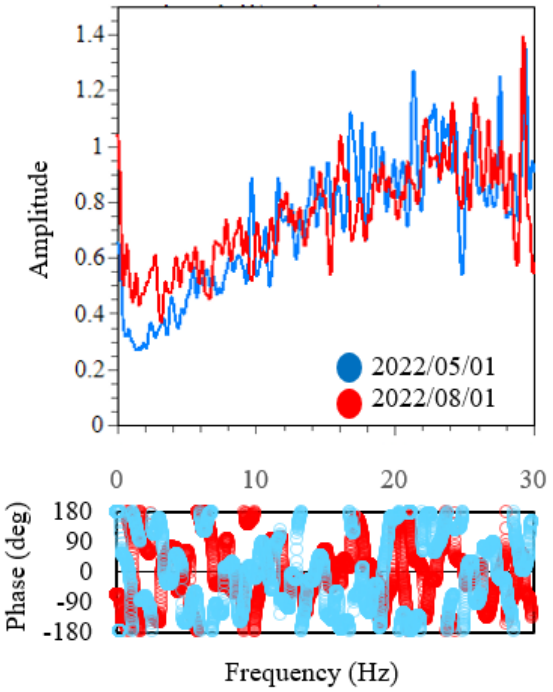

Fig. 11 Fourier amplitude spectrum ratio (upper graph) and Fourier phase spectrum ratio (lower graph)-UD direction

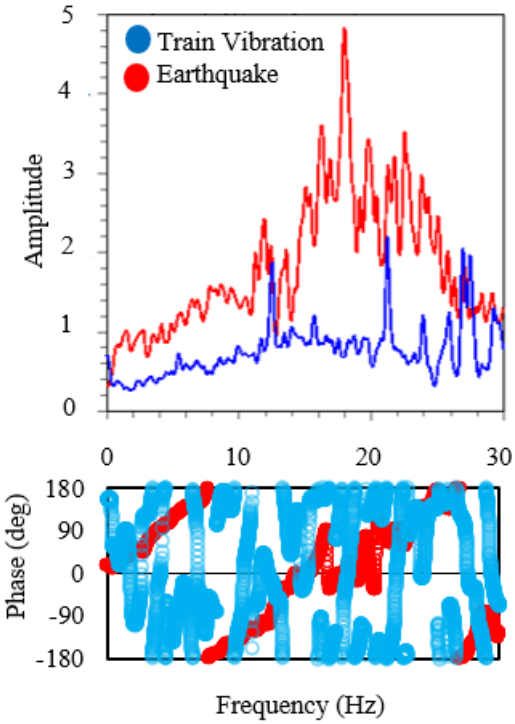

Fig. 12 Fourier amplitude spectrum ratio (upper graph) and Fourier phase spectrum ratio (lower graph)-NS direction

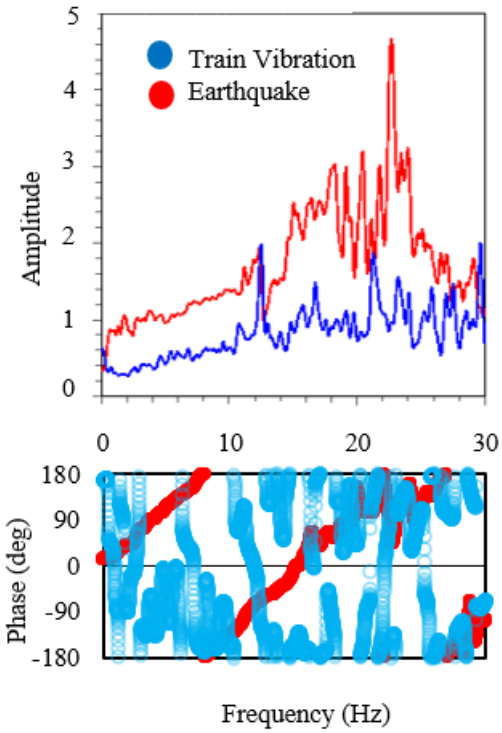

Fig. 13 Fourier amplitude spectrum ratio (upper graph) and Fourier phase spectrum ratio (lower graph)-EW direction

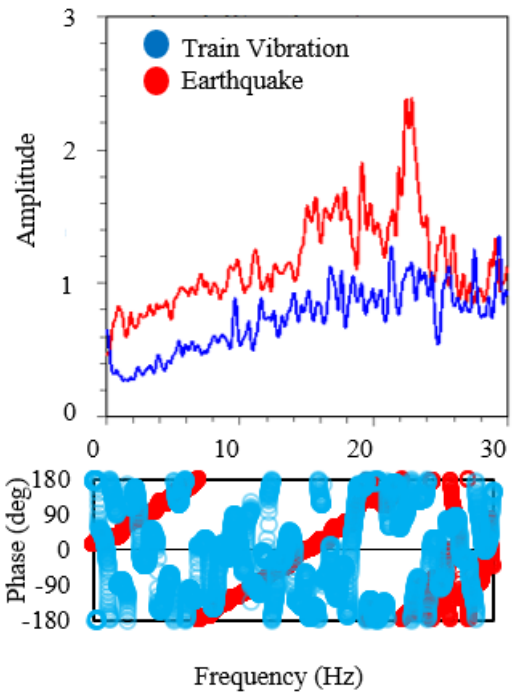

Fig. 14 Fourier amplitude spectrum ratio (upper graph) and Fourier phase spectrum ratio (lower graph)-UD direction

4.3.2 The recorded data from 2022/05/01(Train vibration) and 2023/05/05(2023 Noto earthquake)

Fig. 12-14 shows a comparison of the transfer functions for the NS component (Fig. 12), EW component (Fig. 13), and UD component (Fig. 14) during the train vibrations on May 1, 2022, and the Noto earthquake swarm on May 5, 2023. The upper graphs show the Fourier amplitude spectra, while the lower graphs show the Fourier phase spectra. In the NS component, unlike the previous train vibrations, the retaining wall's natural frequency is clearly observed at 18 Hz. In the EW and UD components, dominant natural frequencies near 22 Hz are also clear. Furthermore, the dynamic amplification ratio (No.2/No.1) for both the NS and EW components is 4.9 times, while for the UD component, it is 2.3 times. When compared to the natural frequencies observed during the train vibrations, some changes were observed, but the natural frequencies did not decrease, indicating no progression of instability.

4.3.3 RMS velocity amplitude ratio

The RMS velocity amplitude ratio is an index that indicates the extent to which the upper part of the retaining wall (the floating stone portion) oscillates relative to the lower part (the foundation portion). It is calculated by taking the vibration records from the floating stone portion and the foundation portion, determining the amplitude's RMS (Root Mean Square) value, and evaluating the ratio between the two. Ogata and Matsuyama and Amano. [11] established a threshold for the danger zone of falling rocks based on the relationship between the resistance force of simulated rolling stones and the RMS velocity amplitude ratio. They categorized an RMS velocity amplitude ratio of 2.0 or higher, corresponding to a resistance force of 3 N/kg or less, as a danger zone for falling rocks. For example, if the RMS velocity ratio is less than 1, the amplitude of the floating stone portion is smaller than that of the foundation portion. Conversely, if the ratio is greater than 1, the amplitude of the floating stone portion is larger than that of the foundation portion. In this study, the retaining wall was first treated as a falling rock using this threshold as a reference, and the risk of retaining wall collapse was evaluated accordingly.

$$R = \frac{\sqrt{\sum_{i=1}^{n} Yi^2/n}}{\sqrt{\sum_{i=1}^{n} Xi^2/n}} \quad (2)$$

R : RMS velocity amplitude ratio, X : Vibration record of the amplitude at the foundation portion, Y: Vibration record of the amplitude at the floating stone portion, n: Number of sampling points

5. EVALUATION OF THE RISK OF RETAINING WALL COLLAPSE

Based on the three vibration characteristics obtained from the above, the risk of retaining wall collapse was assessed. Fig. 15 shows the relationship between the natural frequencies and RMS velocity amplitude ratios for the NS and EW directions. Additionally, the threshold was calculated based on the method by Ogata et al. and is indicated by the dashed line in the figure. There was no observed temporal decline in the natural frequencies of the retaining wall from April 25 to August 1, 2022, when the train vibrations were used as the excitation source. The natural frequency of the retaining wall remained approximately at 12 Hz. Therefore, it can be concluded that there was no risk of destabilization of the retaining wall during the measurement period of train vibrations. During 2023 Noto earthquake on May 5, 2023, the natural frequencies of the retaining wall increased to 18 Hz in the NS direction and 22 Hz in the EW direction. This increase in natural frequency is considered to be due to repair work conducted on the retaining wall after August 2022. However, even though the retaining wall was affected by seismic motion, it was confirmed from the natural frequency that the integrity of the retaining wall was not compromised. The RMS velocity amplitude ratio maintained values less than 1 in April, May, and June, but started showing values close to 1.5 from July. This indicates that the amplitude difference of the vibrations at the upper part of the retaining wall was 1.5 times that of the foundation. A potential cause for this increase could be a reduction in the resistance (friction) at the joint surfaces. Nevertheless, during 2023 Noto earthquake on May 5, 2023, the RMS velocity amplitude ratio was close to 0.5. Thus, it is concluded that the deterioration was not critical for the retaining wall, and its integrity was maintained. Fig. 16 shows the relationship between the damping constant and RMS velocity amplitude ratio for the NS and EW directions. The threshold considered dangerous for the damping constant was set at 0.2 or lower, but the results were significantly below this value. Over the measurement period, it was observed that the damping constant converged to approximately 0.02 to 0.04. According to the Architectural Institute of Japan's "Guidelines for Building Loads and Commentary," the damping constant for concrete structures is considered to be 0.02 to 0.04, similar to the values observed for the retaining wall in this study. From this, it can be concluded that the risk of collapse of the retaining wall due to normal train vibrations and seismic motion from 2023 Noto earthquake is low. During the Noto Peninsula earthquake on January 1, 2024, larger vibrations were observed than those presented

in this study. Although measurements could not be taken due to instrument limitations, further analysis of these larger vibrations is necessary.

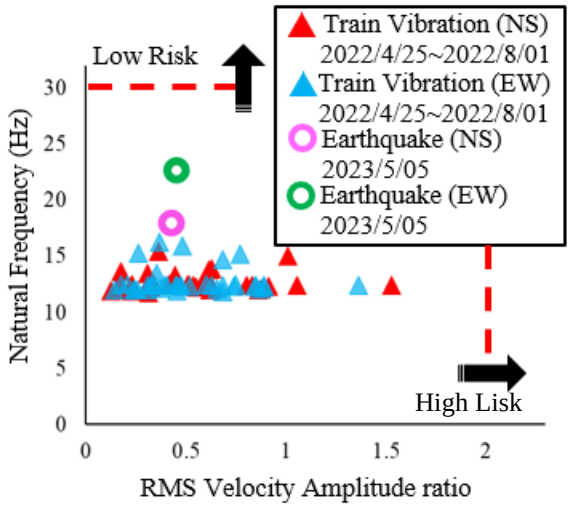

Fig. 15 Collapse Risk Assessment of Retaining Walls (NS direction)

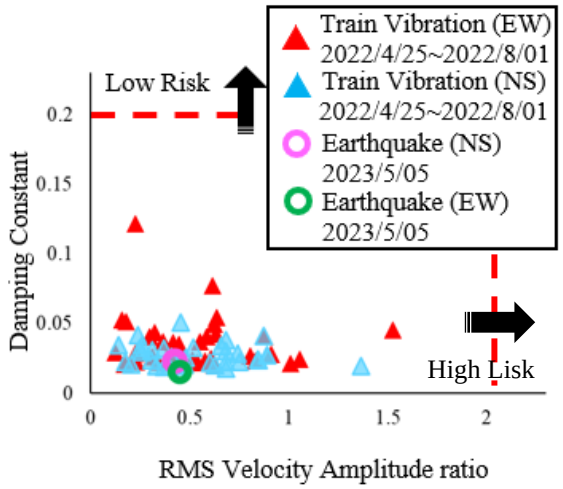

Fig. 16 Collapse Risk Assessment of Retaining Walls (EW direction)

6. CONCLUSION

This study evaluated the collapse risk of the retaining wall using vibration characteristics measured from train-induced vibrations and employing a method to assess the risk of rockfall. The following insights were obtained:

1) The natural frequencies of the retaining wall did not show significant temporal decline during the period of train-induced vibration measurements. Although changes in natural frequencies were observed during the Noto Peninsula earthquake swarm on May 5, 2023, there was no indication of a decrease in values, indicating that instability of the retaining wall is not progressing.
2) The RMS velocity amplitude ratio showed a trend of increasing to near 1.5 around July during the train-induced vibration measurement period. This increase is attributed to decreased resistance (frictional force) to the contact surfaces of construction joints. However, during the Noto Peninsula earthquake swarm on May 5, 2023, the ratio was close to 0.5, suggesting a low risk of collapse for the retaining wall.
3) The damping coefficient was found to fall significantly below the threshold established by previous studies. However, considering that the damping coefficient for concrete structures is typically in the range of 0.02 to 0.04, it cannot be concluded that the damping coefficient of the retaining wall has dropped drastically. Therefore, the integrity of the retaining wall is believed to be maintained.

Based on these points, it is understood that the assessment of deterioration progress and collapse risk of the retaining wall is possible using the three vibration characteristics: natural frequency, damping constant, and RMS velocity amplitude ratio. Currently, data obtained from sensors are temporarily stored on-site and transmitted via LTE lines. In the future, we aim to develop a system that allows real-time monitoring of structural changes from remote locations in conjunction with data collection.

7. ACKNOWLEDGMENTS

Throughout the implementation of this study, we received courteous guidance and valuable advice from Mr. Hashimoto of Chuo Kaihatsu Corporation. We would like to express our sincere gratitude here.

8. REFERENCES

[1] Ministry of Land, Infrastructure, Transport and Tourism, The proportion of social infrastructure that has been in place for over 50 years after construction,https://www.mlit.go.jp/sogoseisaku/maintenance/_pdf/50year_percentage.pdf (Accessed on November 1, 2024)

[2] Inaba T. and Haya H., Overview of soundness diagnosis method for wooden pile foundation piers in railways. Railway Technical Research Institute, Japan Society of Civil Engineers Earthquake Engineering Papers, 2003. pp.1375-1376. (In Japanese)

[3] Nishimura A and Haya H., Method and Example of Determining the soundness of bridge foundations. Railway Technical Research Institute, Earthquake Engineering Research Presentation Lecture Summary, Vol 21, 1991, pp.625-628. (In Japanese)

[4] Nakajima S. and Ehara T. and Abe K., Health diagnosis of old earth retaining walls using vibration characteristics. Railway Technical Research Institute, Railway Research Institute report, Vol 30, Issue 12, 2016, pp.17-22. (In Japanese)

[5] Miyamura M. and Koda Y. and Naito H. and Iwaki I. and Suzuki M., Research on fatigue damage evaluation method for RC deck slabs focusing on vibration characteristics. Structural Engineering Paper Collection, Vol 57A, 2011, pp.1251-1262. (In Japanese)

[6] Fukukawa A. and Hagiwara k. and Takahashi Y. and Kiyono J., Quick Earthquake Damage Evaluation method for RC Piers using Accelerations Measurements, International Journal of GEOMATE, Vol.21(86), 2021, pp.23-31.

[7] Kawano M. and Ichii K. and Takamachi M. and Kurihara O. and Konishi M., Issues on the Ground Health Monitoring of a Retaining Wall using the Microtremor Measurements-From Field Measurement. Japan Geotechnical Society China Branch Paper Report Collection: Ground and Construction, Vol 31, No.1, 2013, pp.195-202. (In Japanese)

[8] Kunii T. Vibration characteristics of embankment ground on sloped land estimated from microtremors. Earthquake Engineering Research Presentation Lecture Summary, Vol 20, pp.149-152, 1989, pp103-108. (In Japanese)

[9] Wan L. and Hashimoto K. and Yamada T. and Kasamatsu K., Measurement of Microtremors and Vibrations of the Ground Using a Small Accelerometer, Vol.69 , No.8 , Ser.No.763 , 2021, pp.37-40. (In Japanese)

[10] Tao S. and Wan L. and Hashimoto K. and Fukuhara M., Stability evaluation of the existing building based on earthquake monitoring, Japanese Geotechnical Society Special Publication, Vol.10, No.36, 2024, pp.1359-1364.

[11] Ogata K. and Matsuyama H. and Amano K., Evaluation of the rockfall potential utilizing the characteristics of vibration. Proceedings of the Japan Society of Civil Engineers, No. 749 VI-61, 2003, pp.123-135. (In Japanese)

[12] Architectural Institute of Japan, General Incorporated Association. Building Load Guidelines and Commentary (2015), 7.2.2 Natural period and damping constant considering the interaction between the building and the ground, 2015, pp.74-424. (In Japanese)

[13] Sakuyama K. and Kitagawa Y., Correspondence of the stiffness-degradation to structural damage. Theoretical and Applied Mechanics Lecture Collection of Lecture Papers, Vol 53, 2004, pp.110-110. (In Japanese)

[14] Nishikawa T. and Arakawa T. and Hisada Y. and Soda S. and Tohdo M. and Yamamura K., Architectural Vibration. Series (Architectural Engineering) 3, Asakura Syoten. 2005. pp.1-120 (In Japanese)

[15] Sano K. and Kikkawa N. and Itoh K. and Suemasa N. and Tanaka T. and Konami T. and Taniyama S., Research on anti-seismic reinforcement method of existing residential dry masonry retaining wall by centrifuge tilting test and 3D DEM, Japanese Geotechnical Society Special Publication, Vol.10, No.18, 2024, pp.627-632.